Journal of the European Ceramic Society xxx (xxxx) xxx–xxx

Contents lists available at ScienceDirect

Journal of the European Ceramic Society

journal homepage: www.elsevier.com/locate/jeurceramsoc

Original Article

The microwave dielectric properties and crystal structure of low temperature sintering $LiNiPO_4$ ceramics

Ping Zhang*, Shanxiao Wu, Mi Xiao*

School of Electrical and Information Engineering and Key Laboratory of Advanced Ceramics and Machining Technology of Ministry of Education, Tianjin University, Tianjin 300072, China

ARTICLE INFO

Keywords:
Microwave dielectric properties
Crystal structure
LTCC
$LiNiPO_4$ ceramics

ABSTRACT

The $LiNiPO_4$ ceramic for the LTCC technology was prepared via the traditional solid-state reaction route and its dielectric properties were investigated for the first time. The best dielectric properties of $LiNiPO_4$ ceramics with a ε_r of 7.18, $Q\times f$ value of 27,754 GHz and τ_f of −67.7 ppm/°C were obtained in samples sintered at 825 °C for 2 h. Rietveld refinement was firstly employed to study the crystal structure and dielectric properties of $LiNiPO_4$ ceramics. Unfortunately, the relatively large negative τ_f was unfavorable to practical applications. Therefore, we introduced TiO_2, which possessed a considerable positive τ_f, to obtain a desired τ_f value. The prepared $LiNiPO_4$ ceramics with 15 wt% TiO_2 sintered at 900 °C for 2 h exhibited excellent dielectric properties of $\varepsilon_r\sim 11.49$, $Q\times f\sim 10{,}792$ GHz, $\tau_f\sim -2.8$ ppm/°C. The Ag co-fired experiments confirmed the excellent chemical compatibility with $LiNiPO_4$-TiO_2 ceramics which might be potential dielectric LTCCs for high frequency applications.

1. Introduction

With the fast development of wireless telecommunication industry, the miniaturization and integration of various components, such as oscillators, antennas and filters, have attracted considerable attentions [1]. Furthermore, the widespread use of mobile communication devices accelerates the study for new technologies to integrate miniaturized dielectric ceramic components [2]. To satisfy the demands for a wide range of practical applications, the low temperature co-fired ceramic (LTCC) technology, one of the most promising integration technologies, has shown its great potential in the production of microwave devices with excellent performances [3]. Therefore, the aspiration for exploiting high quality microwave products is in the process.

Generally, low permittivity (ε_r), high quality factor ($Q\times f$) and near-zero temperature coefficient of resonant frequency (τ_f) are the essential factors of the microwave dielectric materials for the practical applications [4]. In addition, the selected dielectric materials for LTCC technology should have a good chemical compatibility with inexpensive metal silver (Ag) which possesses low conductor loss and low electrical resistance [5].

Recently, owing to the lower melting point of phosphate, some compounds based on phosphorus, such as $LiMPO_4$ (M = Fe, Co, Mn), could be potential LTCC candidates [6]. However, the most studies for $LiMPO_4$ were merely focused on the magnetoelectric and electrochemical properties [6–9]. In 2010, Thomas et al. [2] firstly reported that $LiMgPO_4$ ceramics could be sintered very well at 950 °C for 2 h, which exhibited excellent dielectric properties of $\varepsilon_r\sim 6.6$, $Q\times f\sim 79{,}100$ GHz, $\tau_f\sim -55$ ppm/°C. Later, Hu et al. [10] investigated the dielectric properties of $LiMnPO_4$ ceramics with $\varepsilon_r\sim 8.1$, $Q\times f\sim 44{,}224$ GHz, $\tau_f\sim -90$ ppm/°C. Besides, the $LiMnPO_4$ ceramics could be co-fired with Ag without any chemical reaction. Xia et al. [11] reported the $LiZnPO_4$ ceramics ($\varepsilon_r\sim 5.3$, $Q\times f\sim 28{,}496$ GHz, $\tau_f\sim -80.4$ ppm/°C) that could be as a potential candidate for LTCC applications. To solve stability problems existed in $LiMnPO_4$ system, the TiO_2 was used as an external additive to improve the τ_f value of $LiMnPO_4$ ceramics. Xia et al. [12] reported that $LiMnPO_4$-19 wt%TiO_2 ceramics maintained satisfactory dielectric properties of $\varepsilon_r\sim 12.3$, $Q\times f\sim 38{,}671$ GHz, $\tau_f\sim 6.7$ ppm/°C at 875 °C. However, few studies have reported the dielectric properties and crystal structure of $LiNiPO_4$ ceramics.

In this work, we synthesized the $LiNiPO_4$ ceramics by the traditional solid-state reaction method. The dielectric properties of $LiNiPO_4$ ceramics were systematically studied along with the crystal structure. Moreover, TiO_2 was introduced to adjust the τ_f value to near zero. Meanwhile, the chemical compatibility of $LiNiPO_4$-TiO_2 ceramics with an Ag electrode was discussed. Rietveld refinement was employed to study the crystal structure. What's more, the chemical bond parameters were achieved to investigate the correlation between dielectric properties and crystal structure.

* Corresponding authors.
E-mail addresses: zptai@163.com (P. Zhang), xiaomi@tju.edu.cn (M. Xiao).

https://doi.org/10.1016/j.jeurceramsoc.2018.05.040
Received 11 March 2018; Received in revised form 27 May 2018; Accepted 28 May 2018

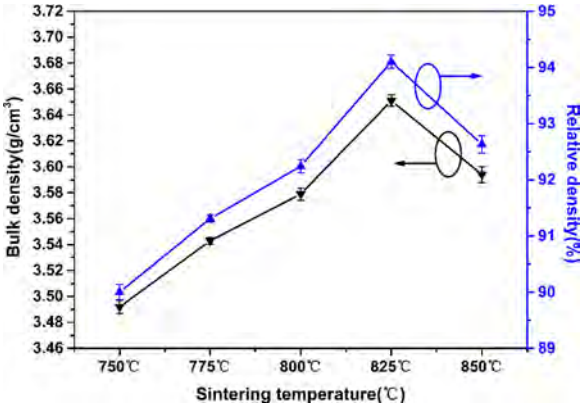

Fig. 1. The variation of bulk and relative densities for $LiNiPO_4$ ceramics.

2. Experimental procedure

The high purity powders of $NH_4H_2PO_4$, Li_2CO_3, NiO and TiO_2 were used as the raw materials. All the starting materials were weighted in accordance with the stoichiometric compositions of $LiNiPO_4$ and ball-milled for 2 h with ethanol. The slurries were dried and sieved with a 40 mesh screen. Afterwards, the obtained samples were first pre-sintered at 550 °C for 2 h followed by a secondary calcination at 700 °C for 4 h. After calcination, the $LiNiPO_4$-x wt% TiO_2 (x = 14, 15, 16, 17) mixtures were prepared by pure $LiNiPO_4$ and TiO_2, and then ball-milled again in ethanol medium for 8 h. After dried, the sieved powders were doped with 8 wt% paraffin as a binder and pressed into cylinders with 15 mm in diameter and 6–7 mm in thickness at 4 MPa. Finally, the obtained cylinders were fired at 550 °C for 2 h to exhaust the binder before sintering at 750–850 °C for 2 h with the heating rate of 3 °C/min.

The phase composition was identified by X-ray diffraction (XRD) (Rigaku D/max 2550 PC, Tokyo, Japan) with Cu Kα radiation (V = 200 kV, I = 40 mA). The diffraction pattern fitting was carried out using the FULLPROF program. The microstructures of the sintered samples polished and thermally etched were observed by a scanning electron microscopy (SEM) (ZEISS MERLIN Compact, Germany). The composition analysis was performed using an energy-dispersive X-ray spectroscopy (EDXS) (Genesis MT XV 60) attached to the SEM.

The microwave dielectric properties of the sintered samples were measured in the frequency range of 7–13 GHz with a network analyzer

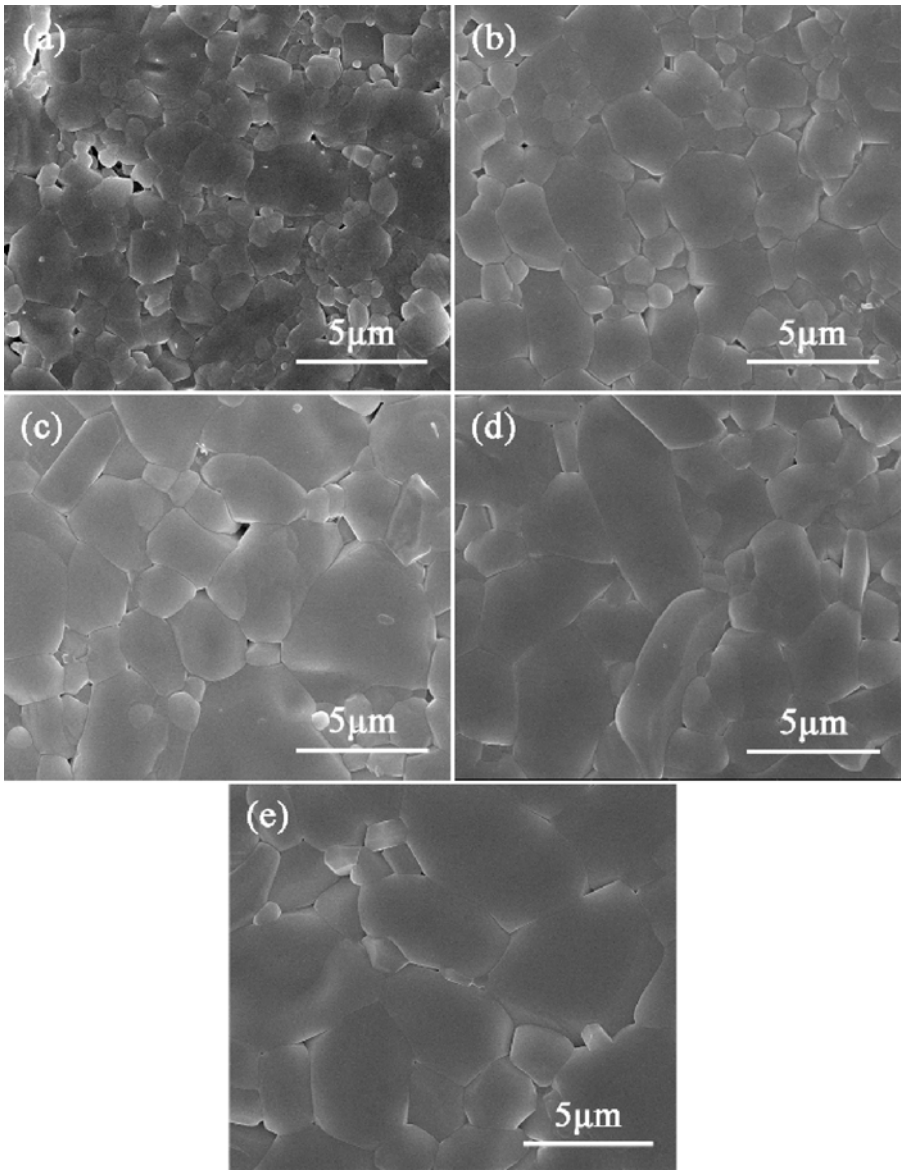

Fig. 2. The SEM micrographs of $LiNiPO_4$ ceramics sintered at various temperatures for 2 h: (a) 750 °C, (b) 775 °C, (c) 800 °C, (d) 825 °C, (e) 850 °C.

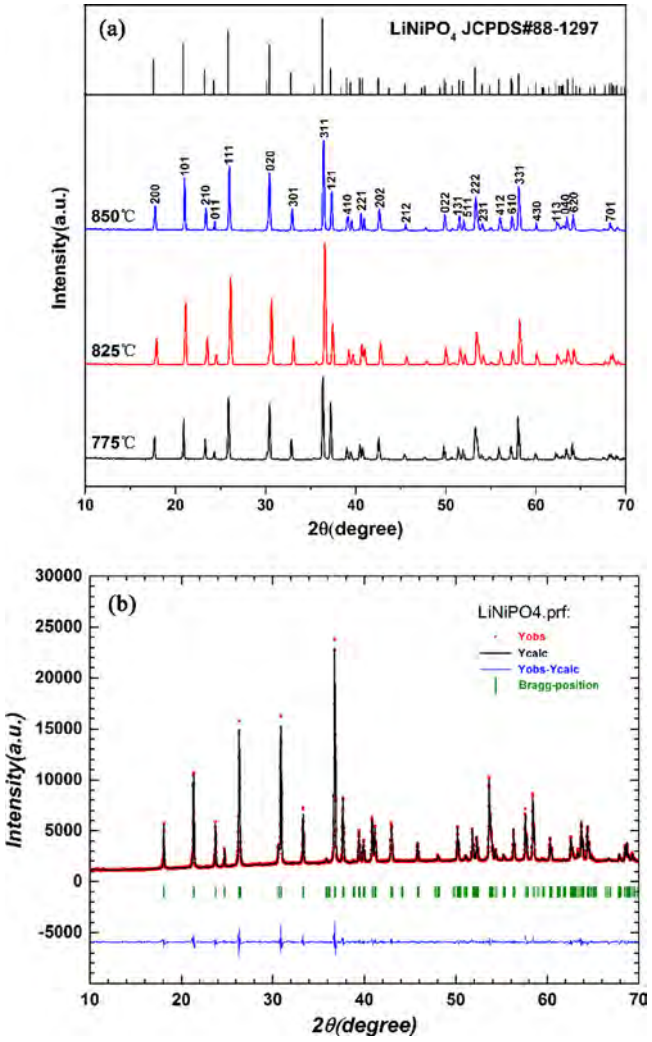

Fig. 3. (a) The XRD patterns of $LiNiPO_4$ ceramics sintered at various temperatures for 2 h, and (b) structural refinement patterns of $LiNiPO_4$ ceramics sintered at 825 °C for 2 h.

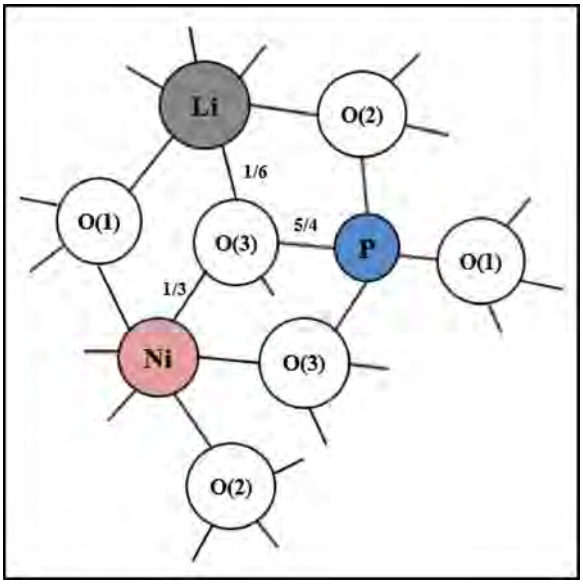

Fig. 4. The coordination number and charge distribution of ions in $LiNiPO_4$ ceramics.

(N5234A, Agilent Co., America). The permittivity was measured using Hakki-Coleman method by exciting the TE_{011} resonant mode of dielectric resonator [13]. The quality factor values were measured using the TE_{01d} mode by the shielded cavity method [14]. Temperature coefficient of resonant frequency was measured in the temperature range from 25 °C to 85 °C. It was obtained by the following formula:

$$\tau_f = \frac{f_2 - f_1}{f_1(T_2 - T_1)} \times 10^6 (ppm/°C) \quad (1)$$

where f_1 and f_2 represented the corresponding frequency at the temperature of T_1 and T_2 respectively.

The bulk densities were measured by the Archimedes method. The theoretical density was obtained as follows:

$$\rho_{theory} = \frac{ZA}{V_C N_A} \quad (2)$$

where Z, A, V_C and N_A were number of atoms in the unit cell, atomic weight (g/mol), volume of unit cell (cm^3), and Avogadro constant (mol^{-1}), respectively. The relative density was defined by Eq. (3):

$$\rho_{relative} = \frac{\rho_{bulk}}{\rho_{theory}} \times 100\% \quad (3)$$

3. Results and discussions

Fig. 1 showed the variation of bulk and relative densities for $LiNiPO_4$ ceramics sintered at the range of 750–850 °C. The theoretical density of $LiNiPO_4$ ceramics was calculated to 3.881 g/cm^3. Obviously, higher sintering temperature would result in a denser sample, because the grains grew faster and more pores would be removed at a higher temperature. The maximum value of relative density with 94.1% was achieved at 825 °C, then a slight decreasing tendency with a further increased temperature. The initial density with a relatively low value was mainly due to the insufficient grain growth and many pores were still left inside of the samples. When rising the sintering temperature, the thermodynamic effects drove the smaller grain to the bigger one and more and more pores were removed from the ceramic samples. However, excessive sintering temperature would result in abnormal grain growth and lots of pores couldn't get out from the grains, which eventually led to a decline in relative density. The details about the direct change of density and pores would be discussed in the following SEM analysis.

The SEM micrographs of $LiNiPO_4$ ceramics at various temperatures for 2 h were given in Fig. 2. It was easily found that the grains didn't grow well, which presented undense microstructure and many pores still existed at 750 °C shown in Fig. 2(a). From Fig. 2(b)–(e), with a continuously increasing of sintering temperature, the pores gradually decreased and the grain size increased correspondingly. When the temperature rose to 825 °C, well-distributed and dense microstructures could be formed and the average grain size was around 3–5 μm, as presented in Fig. 2(d). With the temperature further increased to 850 °C, some grains appeared excessive growth shown in Fig. 2(e). It was quite simple to generate built-in pores which were not conductive to the dielectric properties of ceramic samples. The discussion of above SEM micrographs was consistent with the density analysis, which confirmed that the morphology of $LiNiPO_4$ ceramics was stronger influenced by the sintering temperature.

Fig. 3(a) presented the XRD patterns of $LiNiPO_4$ ceramics at various temperatures for 2 h. All the peaks of specimens matched with the standard PDF card (JCPDS #88-1297) of $LiNiPO_4$ phase without any additional phase in all range. The structural refinement patterns of $LiNiPO_4$ ceramics sintered at 825 °C for 2 h were depicted in Fig. 3(b), where the blue line signified the discrepancy between the calculated and observed intensities, the green short vertical lines marked Bragg reflections positions. The reliability of refinement results was given by the reliability factor of patterns (R_p) and reliability factor of weighted

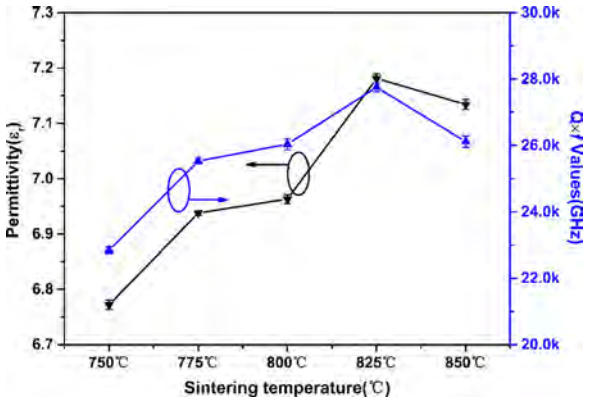

Fig. 5. The permittivity (ε_r) and $Q\times f$ values of $LiNiPO_4$ ceramics with the sintering temperatures.

patterns (R_{wp}). The consequences could be acceptable only if the R_p and R_{wp} were less than 15%. The orthorhombic structured $LiNiPO_4$ ceramics belonged to the *Pnma* space group. The refined lattice parameters in $LiNiPO_4$ ceramics were a = 10.0251 Å, b = 5.8596 Å, c = 4.6762 Å and V = 274.69 Å^3, the discrepancy factors were R_p = 14.0% and R_{wp} = 11.8% which could be accepted. Four $LiNiPO_4$ molecules were contained in per unit cell. The A-site (Li^+, Ni^{2+}) cations that occupied the 4a and 4c Wyckoff positions were octahedrally coordinated with oxygen anions and B-site (P^{5+}) cation occupying the 4c Wyckoff position was tetrahedrally coordinated with oxygen anions.

In order to get a deep insight about the dielectric properties and structural characteristics, the complex chemical bond theory was firstly employed to study the $LiNiPO_4$ ceramics. In our previous works, we have successfully solved many problems about the correlation between dielectric properties and crystal structure for some complex compounds, like $NdNbO_4$ [15,16]. Atomic coordination and all bond lengths were obtained from the Rietveld refinement results (Supplementary Information, Table S1). In the $LiNiPO_4$ system, there were three types of oxygen anions which were differentiated into O(1), O(2) and O(3). On the basis of the structural data and the complex chemical bond theory, the $LiNiPO_4$ compounds could be decomposed as follows:

$$LiNiPO_4 = LiNiPO(1)O(2)O(3)_2$$
$$= Li_{1/3}O(1)_{1/2} + Li_{1/3}O(2)_{1/2} + Li_{1/3}O(3)_{1/2} + Ni_{1/6}O(1)_{1/4} + Ni_{1/6}O(2)_{1/4} + Ni_{2/3}O(3) + P_{1/4}O(1)_{1/4} + P_{1/4}O(2)_{1/4} + P_{1/}O(3)_{1/2}$$
$$= Li_{1/3}O(1)_{1/2} + Li_{1/3}O(2)_{1/2} + Li_{1/3}O(3)_{1/2} + Ni_{1/6}O(1)_{1/4} + Ni_{1/6}O(2)_{1/4} + Ni_{1/3}O(3)^1_{1/2} + Ni_{1/3}O(3)^2_{1/2} + P_{1/4}O(1)_{1/4} + P_{1/4}O(2)_{1/4} + P_{1/}O(3)_{1/2}$$

The coordination number and charge distribution of ions in the $LiNiPO_4$ ceramics were shown in Fig. 4. The effective valence electron numbers of Li, Ni, P cations were Z_{Li} = 1, Z_{Ni} = 2 and Z_P = 5. And in each type bond, the effective valence electron numbers of O anions were different. Specifically, $Z_O = -2/3$ in Li—O bond, $Z_O = -4/3$ in Ni—O bond and $Z_O = -5$ in P—O bond.

The permittivities of $LiNiPO_4$ ceramics with sintering temperatures were depicted in Fig. 5. It could be easily found that the permittivity firstly ascended to a maximum value of 7.18 at 825 °C, and then had a descending. The variation tendency of ε_r was approximate to that of density. Ordinarily, the permittivity of ceramics mainly depended on the intrinsic parameters, such as polarizability, and extrinsic parameters, such as porosity and secondary phase [17]. In this paper, the permittivity depended on the density and dielectric polarizability because of no second phase existed. Furthermore, as the specimens had a high relative density (> 94% at 825 °C), the dielectric polarizability played a more important role in affecting the permittivity. The theoretical dielectric polarizability (α_{theo}) of $LiNiPO_4$ ceramics was calculated to be 11.69 based on the Shannon additive rule as follows:

$$\alpha_{theo}(LiNiPO_4) = \alpha(Li^+) + \alpha(Ni^{2+}) + \alpha(P^{5+}) + 4\alpha(O^{2-}) \quad (4)$$

where $\alpha(Li^+)$ = 1.20 Å^3, $\alpha(Ni^{2+})$ = 1.23 Å^3, $\alpha(P^{5+})$ = 1.22 Å^3 and $\alpha(O^{2-})$ = 2.01 Å^3 were reported by Shannon [18]. The observed dielectric polarizability (α_{obs}) was calculated to be 11.04 according to the Clausius-Mossotti equation in Eq. (5) based on the measured permittivity.

$$\alpha_{obs} = \frac{1}{b} V_m \frac{\varepsilon_r - 1}{\varepsilon_r + 2} \quad (5)$$

where b, V_m and ε_r represented constant value ($4\pi/3$), the molar volume of specimens and the measured permittivity, respectively. It could be found that the value of observed dielectric polarizability (α_{obs}) was approximate to that of the theoretical dielectric polarizability (α_{theo}).

It was easily known that the dielectric polarizability was in proportion to the bond ionicity, so there was an inherent connection between permittivity and bond ionicity [19] (Supplementary Information, Section 1). Fig. 6(a) plotted the corresponding graph of bond ionicity f_i (A/B—O) with the variation of A/B—O bonds and the detailed information of calculated results could be found in Table S2. The order of bond ionicity was f_i (Ni—O) > f_i (P—O) > f_i (Li—O) observed in Fig. 6(a) and the results indicated that the bond ionicity f_i (Ni—O) made a more significant contribution to the permittivity of $LiNiPO_4$ ceramics.

The $Q\times f$ values of $LiNiPO_4$ ceramics with the sintering temperatures were also given in Fig. 5. It was seen that the $Q\times f$ value rose and reached a maximal value of 27,754 GHz at 825 ℃, then showed a downward trend, which was consistent with that of the density. On the basis of SEM results exhibited in Fig. 2(a)–(d), the higher $Q\times f$ value was mainly due to the less porosity. Further high temperature would bring about irregular micromorphology, which was very bad for the $Q\times f$ values.

Based on the complex chemical bond theory, the lattice energy was employed to analyze the theoretical factor of the $Q\times f$ value [20] (Supplementary Information, Section 2). Table S2 also presented the calculated results of lattice energy and the graph of lattice energy U_{cal}

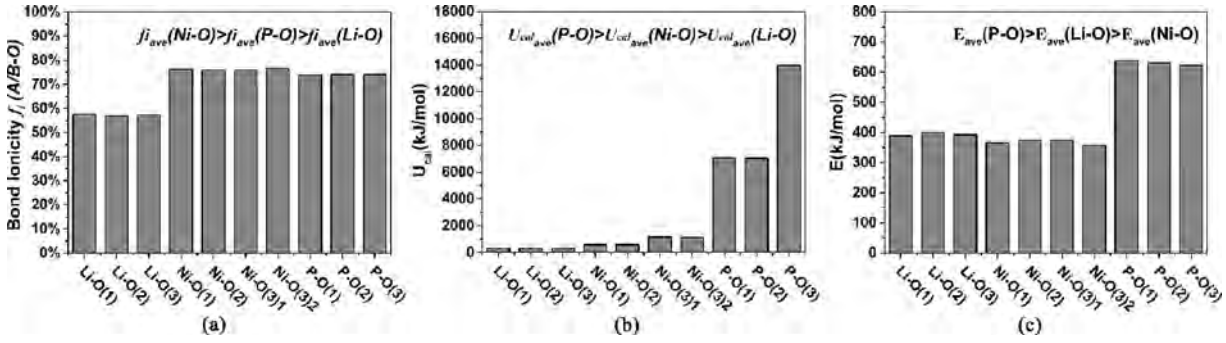

Fig. 6. (a) Bond ionicity of f_i (A/B—O) with the variation of A/B—O bonds in $LiNiPO_4$ ceramics, (b) Lattice energy of U_{cal}(A/B—O) with the variation of A/B—O bonds in $LiNiPO_4$ ceramics, and (c) Bond energy of E with the variation of A/B—O bonds in $LiNiPO_4$ ceramics.

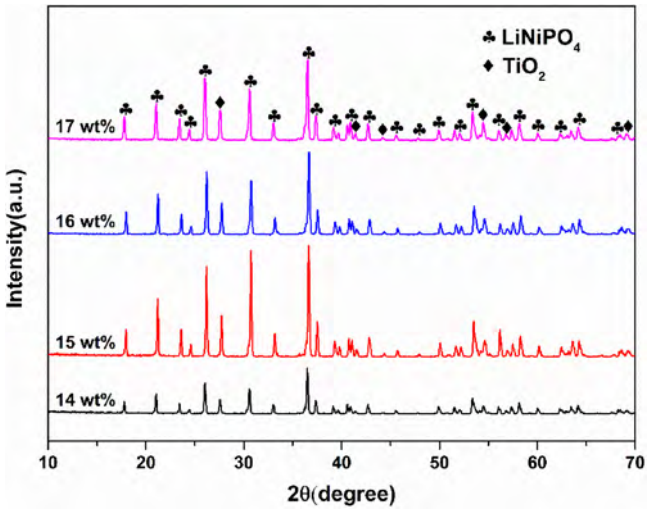

Fig. 7. The XRD patterns of $LiNiPO_4$-x wt%TiO_2 (x = 14, 15, 16, 17) ceramics sintered at 900 °C for 2 h.

(A/B–O) with the variation of A/B–O bonds in $LiNiPO_4$ samples was depicted in Fig. 6(b). The concept of the lattice energy was defined as the heat of dissociation of one mole of solid into its structural components, which could be employed to evaluate the phase stability of a crystal structure [21]. It was calculated that the average values of lattice energy for U_{cal} (Li—O), U_{cal} (Ni—O) and U_{cal} (P—O) were 329, 845 and 9352 kJ/mol, respectively. Due to the sequence of U_{cal} (P—O) > U_{cal} (Ni—O) > U_{cal} (Li—O), the U_{cal} (P—O) made dominating effects on the $Q \times f$ values for $LiNiPO_4$ ceramics. It was proposed that the $Q \times f$ values of $LiNiPO_4$ samples could be concluded by the changes of lattice energy, especially the lattice energy of P—O bonds. The larger lattice energy was, the higher $Q \times f$ value was.

Furthermore, as we all known, the shorter bond length was relevant to the higher bond energy [22] which signified that a crystal structure owns better stability. Based on the electronegativity and bond energy theory reported by R. T. Sanderson, the bond energy of a complex crystal could be obtained [23,24] (Supplementary Information, Section 3). The corresponding image of bond energy E with the variation of A/B—O bonds was depicted in Fig. 6(c) based on the calculated data listed in Table S3. The average values of bond energy E were 399.003, 365.232 and 627.584, for Li—O, Ni—O and P—O bonds, respectively. As a result of the sequence about bond energy of E (P—O) > E (Li—O) > E (Ni—O), it could be easily observed that the bond energy of P—O bonds also played a crucial role in the $LiNiPO_4$ ceramics for $Q \times f$ values.

For the practical applications, the stability (a nearly zero τ_f) came to the first position. However, we didn't obtain a desirable τ_f for $LiNiPO_4$ ceramics. Therefore, TiO_2 was introduced to optimize the τ_f values of $LiNiPO_4$ ceramics. Fig. 7 presented the XRD patterns of $LiNiPO_4$-x wt%TiO_2 ceramics sintered at 900 °C for 2 h. It could be found that $LiNiPO_4$ (PDF#88-1297) coexisted with TiO_2 (PDF#21-1276) and no additional phase was detected. This meant that there was no chemical reaction between $LiNiPO_4$ and TiO_2. It was guessed that there was a significant difference in the crystal structure of both substances so that the chemical reaction was limited [25].

Fig. 8 exhibited the SEM images of $LiNiPO_4$-x wt%TiO_2 ceramics sintered at 900 °C for 2 h. It was observed that all specimens containing TiO_2 displayed a significant difference in surface structures compared with the samples without TiO_2 in Fig. 2. Overall, the samples showed a relatively dense microstructure, but the introduction of TiO_2 had some adverse effects on the density. It was obvious that there were two substances observed separately. The conclusion obtained from this part was consistent with the XRD images shown in Fig. 7. Owing to the high sintering temperature of TiO_2 about 1500 °C [2], the ions' diffusion rate of the new compounds would be relatively slow at the lower sintering

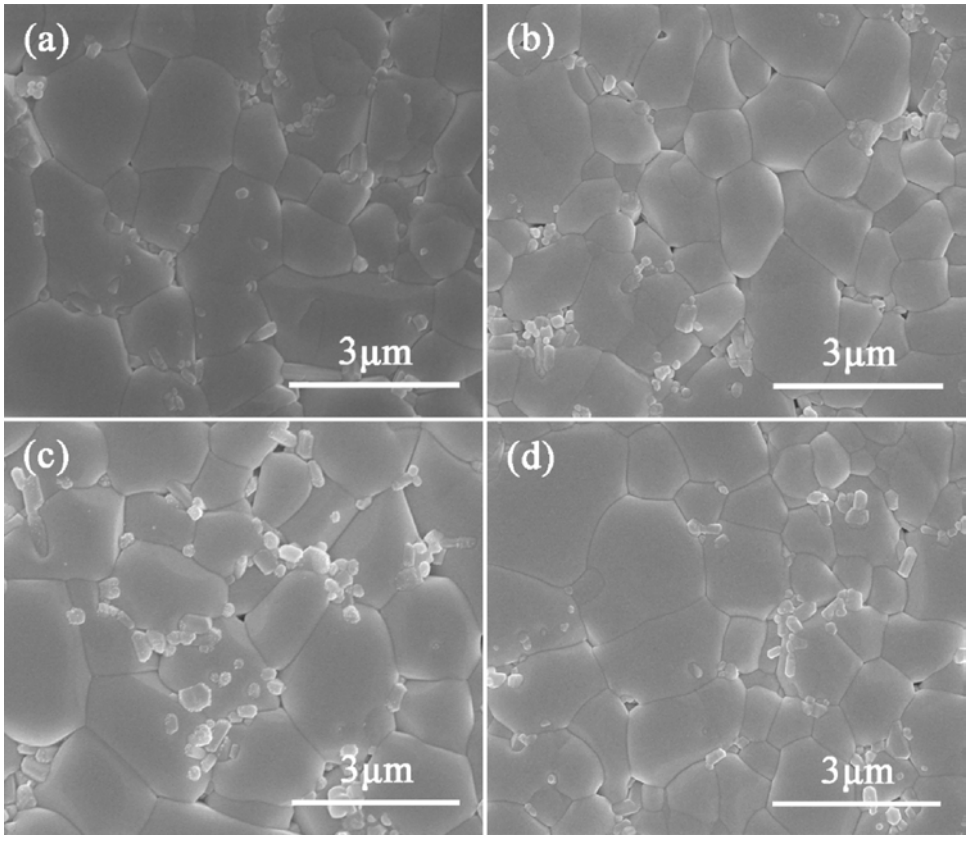

Fig. 8. The SEM images of $LiNiPO_4$-x wt%TiO_2 ceramics sintered at 900 °C for 2 h: (a) x = 14, (b) x = 15, (c) x = 16, (d) x = 17.

Table 1
Dielectric properties of $LiNiPO_4$-x wt%TiO_2 ceramics sintered at 900 °C for 2 h.

x	ε_r	$Q \times f$ (GHz)	τ_f (ppm/°C)
0	7.18	27,754	−67.7
14	10.95	11,676	−9.9
15	11.49	10,792	−2.8
16	11.58	10,522	+3.1
17	12.29	10,723	+8.8

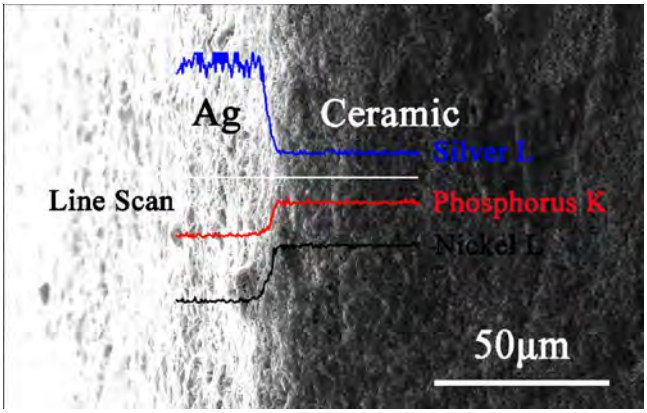

Fig. 9. The EDXS analysis of $LiNiPO_4$-15 wt% TiO_2 ceramics co-fired with Ag electrode at 900 °C for 2 h.

temperature. It could be supposed that the mixture of TiO_2 made the temperature upward and changed the grain morphology.

The dielectric properties of $LiNiPO_4$-x wt%TiO_2 ceramics as a function of x value sintered at 900 °C for 2 h were listed in Table 1. With the increment of TiO_2 content, the permittivity and τ_f of the samples gradually increased, which was probably owing to that TiO_2 had a larger ε_r (~100) and a large positive τ_f [26]. Overall, the $Q \times f$ values showed a downward tendency with the increase of TiO_2 content, which was perhaps because of the non-uniform mixing of phases leading to adverse effects on $Q \times f$ values as shown in Fig. 8 [2,27]. What's more, as a result of the higher sintering temperature of TiO_2, the samples with various amounts of TiO_2 might not be sufficiently densified at a relatively low firing temperature, so that the $Q \times f$ values decreased in a certain extent. The τ_f increased from −67.7 to +8.8 ppm/°C. It was found that near zero τ_f could be obtained by tuning the amount of TiO_2 and the $LiNiPO_4$ with 15 wt% TiO_2 displayed a good value of $\tau_f \sim -2.8$ ppm/°C.

Fig. 9 showed the EDXS line scanning analysis of the interface between the Ag electrode and the $LiNiPO_4$-15 wt% TiO_2 ceramics. It was observed that the Ag profile declined sharply at the interface, which indicated that Ag didn't diffuse into the ceramics during the co-firing process. Correspondingly, there were low amount of Ni and P in the Ag electrode which also suggested that there was no chemical reaction taken place at the interface. In conclusion, the $LiNiPO_4$ ceramics with 15 wt% TiO_2 were chemically compatible with Ag. Therefore, $LiNiPO_4$ ceramic with TiO_2 could be a potential material for LTCC applications.

4. Conclusion

In this paper, the dielectric properties and crystal structure of $LiNiPO_4$ ceramics were systematically investigated. The well dense samples sintered at 825 °C for 2 h exhibited good dielectric properties of $\varepsilon_r \sim 7.18$, $Q \times f \sim 27{,}754$ GHz, $\tau_f \sim -67.7$ ppm/°C. Based on the complex chemical bond theory, the bond ionicity f_i (Ni-O) made a more significant contribution to the permittivity and the lattice energy and bond energy of P—O bonds played the crucial roles for $Q \times f$ values in comparison with Li—O and Ni—O bonds. The τ_f was tuned to near zero with the addition of TiO_2. Especially, the $LiNiPO_4$ with 15 wt% TiO_2 sintered at 900 °C for 2 h still maintained satisfactory performance with $\varepsilon_r \sim 11.49$, $Q \times f \sim 10{,}792$ GHz, $\tau_f \sim -2.8$ ppm/°C and also showed great chemical compatibility with the commonly used Ag electrode. Overall, the $LiNiPO_4$ ceramic could be a promising candidate for LTCC applications.

Acknowledgment

This work was supported by the National Natural Science Foundation of China (No. 61671323).

Appendix A. Supplementary data

Supplementary material related to this article can be found, in the online version, at doi: https://doi.org/10.1016/j.jeurceramsoc.2018.05.040.

References

[1] W. Wersing, Microwave ceramics for resonators and filters, Curr. Opin. Solid St. M. 1 (1996) 715–731.
[2] D. Thomas, M.T. Sebastian, Temperature-compensated $LiMgPO_4$: a new glass-free low-temperature cofired ceramic, J. Am. Ceram. Soc. 93 (2010) 3828–3831.
[3] H. Jantunen, T. Kangasvieri, J. Vähäkangas, S. Leppävuori, Design aspects of microwave components with LTCC technique, J. Eur. Ceram. Soc. 23 (2003) 2541–2548.
[4] M.T. Sebastian, H. Jantunen, Low loss dielectric materials for LTCC applications: a review, Int. Mater. Rev. 53 (2008) 57–90.
[5] M.T. Sebastian, Dielectric Materials for Wireless Communication, Elsevier, Amsterdam, 2008, pp. 1–3.
[6] J.O. Herrera, H. Camacho-Montes, L.E. Fuentes, L. Álvarez-Contreras, $LiMnPO_4$: review on synthesis and electrochemical properties, J. Mater. Sci. Chem. Eng. 3 (2015) 54–64.
[7] D. Vaknin, J.L. Zarestky, J.P. Rivera, H. Schmid, Commensurate-incommensurate magnetic phase transition in magnetoelectric single crystal $LiNiPO_4$, Phys. Rev. Lett. 92 (2004) 207201.
[8] M. Minakshi, P. Singh, D. Appadoo, D.E. Martin, Synthesis and characterization of olivine $LiNiPO_4$ for aqueous rechargeable battery, Electrochim. Acta 56 (2011) 4356–4360.
[9] I. Kornev, M. Bichurin, J.P. Rivera, S. Gentil, H. Schmid, A.G.M. Jansen, P. Wyder, Magnetoelectric properties of $LiCoPO_4$ and $LiNiPO_4$, Phys. Rev. B 62 (2000) 12247–12253.
[10] X. Hu, Z.F. Cheng, Y. Li, Z.Y. Ling, Dielectric relaxation and microwave dielectric properties of low temperature sintering $LiMnPO_4$ ceramics, J. Alloys Compd. 651 (2015) 290–293.
[11] C.C. Xia, D.H. Jiang, G.H. Chen, Y. Luo, B. Li, C.L. Yuan, C.R. Zhou, Microwave dielectric ceramic of $LiZnPO_4$ for LTCC applications, J. Mater. Sci. Mater. Electron. 28 (2017) 12026–12031.
[12] C.C. Xia, G.H. Chen, C.L. Yuan, C.R. Zhou, Low-temperature co-fired $LiMnPO_4$-TiO_2 ceramics with near-zero temperature coefficient of resonant frequency, J. Mater. Sci. Mater. Electron. 28 (2017) 13970–13975.
[13] B.W. Hakki, P.D. Coleman, A dielectric resonator method of measuring inductive capacities in the millimeter range, IEEE Trans. Microw. Theory Tech. 8 (1960) 402–410.
[14] W.E. Courtney, Analysis and evaluation of a method of measuring the complex permittivity and permeability microwave insulators, IEEE Trans. Microw. Theory Tech. 18 (1970) 476–485.
[15] P. Zhang, Y.G. Zhao, L.X. Li, The correlations among bond ionicity, lattice energy and microwave dielectric properties of $(Nd_{1-x}La_x)NbO_4$ ceramics, Phys. Chem. Chem. Phys. 17 (2015) 16692–16698.
[16] P. Zhang, Y.G. Zhao, J. Liu, Z.K. Song, M. Xiao, X.Y. Wang, Correlation of crystal structure and microwave dielectric properties of $Nd_{1.02}(Nb_{1-x}Ta_x)_{0.988}O_4$ ceramic, Dalton. Trans. 44 (2015) 5053–5057.
[17] H.L. Pan, L. Cheng, H.T. Wu, Relationships between crystal structure and microwave dielectric properties of $Li_2(Mg_{1-x}Co_x)_3TiO_6$ ($0 \le x \le 0.4$) ceramics, Ceram. Int. 43 (2017) 15018–15026.
[18] R.D. Shannon, Dielectric polarizabilities of ions in oxides and fluorides, J. Appl. Phys. 73 (1993) 348–366.
[19] Q.B. Meng, Z.J. Wu, S.Y. Zhang, Dependence of superconducting temperature on chemical bond parameters in $YBa_2Cu_3O_{6+\delta}$ ($\delta = 0-1$), J. Phys. Chem. Solids 59 (1998) 633–639.
[20] P. Zhang, Y.G. Zhao, Effects of structural characteristics on microwave dielectric properties of $Li_2Mg(Ti_{1-x}Mn_x)_3O_8$ ceramics, J. Alloys Comp. 647 (2015) 386–391.
[21] W.S. Xia, L.X. Li, P.F. Ning, Q.W. Liao, Relationship between bond ionicity, lattice energy, and microwave dielectric properties of $Zn(Ta_{1-x}Nb_x)_2O_6$ ceramics, J. Am. Ceram. Soc. 95 (2012) 2587–2592.
[22] P. Zhang, Y.G. Zhao, H.T. Wu, Bond ionicity, lattice energy, bond energy and microwave dielectric properties of $ZnZr(Nb_{1-x}A_x)_2O_8$ (A = Ta, Sb) ceramics, Dalton Trans. 44 (2015) 16684–16693.

[23] R.T. Sanderson, Multiple and single bond energies in inorganic molecules, J. Inorg. Nucl. Chem. 30 (1968) 375–393.
[24] R.T. Sanderson, Electronegativity and bond energy, J. Am. Chem. Soc. 105 (1983) 2259–2261.
[25] G.H. Chen, M.Z. Hou, B. Yao, C.L. Yuan, C.R. Zhou, H.R. Xu, Silver co-firable $Li_2ZnTi_3O_8$ microwave dielectric ceramics with LZB glass additive and TiO_2 dopant, Int. J. Appl. Ceram. Tech. 10 (2013) 492–501.
[26] Z.W. Dong, Y. Zheng, P. Cheng, X.P. Lv, W. Zhou, Microwave dielectric properties of $Li(Mg_{1-x}Ni_x)PO_4$ ceramics for LTCC applications, Ceram. Int. 40 (2014) 12983–12988.
[27] C.H. Hsu, H.A. Ho, Microwave dielectric in the $Sm(Co_{1/2}Ti_{1/2})O_3$-$CaTiO_3$ ceramic system with near-zero temperature coefficient with resonant frequency, Mater. Lett. 64 (2010) 396–398.